Computation of the Liquid Scintillation Counting Efficiency for K-L Electron Capture Radionuclide Using Viaskl

Habiba Garba Ahmad and F.S. Koki

Department of Physics, Bayero University, Kano

Abstract

This paper uses the program VIASKL to compute the liquid scintillation counting efficiency for ^{55}Fe (K-L shell). The counting efficiency was calculated as a function of the figure of merit using a model based on an in-depth analysis of the detection processes involved. The contribution of X-rays and Auger transitions to the 21 atomic rearrangement pathway is taken into account and the efficiency for each figure of merit as a weighted sum over the 21 terms is obtained using different types of scintillators and vial sizes. For each nuclide the capture probability, fluorescence yield, Auger transitions (for KLL, KLM, KMM and LMM), X-ray transition (KL, KM, and LM) were computed. Energies and intensities for each of the transitions were also computed. The energy of the auger transition was computed to be approximately equal to 220.3797KeV and the auger intensity was computed to be approximately equal to77.6042 counts per minute while the X-ray transition energy was approximately computed to be 3711.477KeV and the X-ray transition intensity was computed as 265.5065counts per minute. The average liquid scintillation counting efficiency of ^{55}Fe was calculated to be 46.67% and the figure of merit computed to be 1.5064.This result was compared with reported computed liquid scintillation counting efficiency of 47.5354% with a figure of merit equal to 1.4679.

1.0   Introduction

Electron capture (EC) nuclides can be accurately measured by liquid scintillation counting if the detection efficiency is well known [1]. Liquid scintillation techniques can be used for radionuclide standardization when the calculation of detection efficiency is possible [2].Liquid scintillation counting is a laboratory method in life sciences for measuring radiation from beta-emitting nuclides [3]. It is commonly used for measuring radioactive isotopes e.g. Tritium (^{3}H) and carbon -14 (^{14}C) which emit beta or corresponding particles [4]. Compared to other methods of radioactivity measurement, the liquid scintillation technique have remarkable advantage that radiations can be measured without self absorption, external absorption and scattering under 4π geometry [5]. This advantage leads to an accurate radiation measurement with a high counting efficiency. Nevertheless, other perturbation phenomenon can arise. The most important of them is the quenching which refers to any factor which results in the loss of photon emission from the sample to be measured [5].

Liquid scintillation counting is capable of detecting all types of nuclear decays making it an attractive waste appraiser [6]. It is particularly suited for detecting nuclides that decay by $\propto$ and $\beta\pm$ emission. Some nuclides decay by electron capture (EC), but even these emit detectable Auger electrons andX-rays. Also any accompanying γ-rays and conversion electrons (CE) emissions may be detected [6].

In radionuclide metrology, liquid scintillation counting (LSC) is widely used for the activity standardization of electron capture, pure beta and alpha nuclide [7].

Corresponding author: H. G. Ahmad, E-mail: habibagarba36@gmail.com, Tel.: +2348065882257 & 08064120841(F.S.K)

In liquid scintillation counting, the terms counting efficiency and quenching are synonymous and the counting efficiency of the counting system must be determined [7]. These calculations are based on statistical and physical models of the source and the detector and require the calculation of the energy transferred to the scintillator, which is generally taken as the electron spectrum emitted by the measured nuclide [8].

1.2 Liquid Scintillators

A liquid scintillator (LS) converts a fraction of the energy of ionizing radiation into light. It basically consists of scintillator molecules dissolved in an organic solvent [8]. Other components are also added (secondary solvent, secondary scintillator, surfactant, extractant, and quencher) to adapt the LS cocktail to particular uses [9]. The liquid scintillation cocktail composition should enable efficient transfer of energy between the solvent and the scinitillator solute as well as coexistence of the aqueous radioactive solution with the organic solvent [10].

The solvent is the main components of the cocktail and its main purpose is to absorb the energy of charged particles emitted by radionuclide and to propagate this energy to the fluorescence molecules [11]. Benzene and Toluene are used as scintillants, but less toxic solvents like xylene or pseudocumene are now preferred.

Radionuclide decay radiation passes through the liquid scintillator, interacting mainly with solvent molecules [11].

Incident electrons, or secondary electrons created by the interaction of radiation with matter excite or ionize solvent molecules but most of the incident energy is dissipated as heat [9].

Quenching is used to describe various physical or chemical processes which reduce the light output of the scintillator [8]. Chemical or impurity quenching is caused by the presence of added substances acting as chemical scavengers of excited molecules of the solvent, leading to the production of heat instead of light. The scale of the chemical quenching depends on the lifetime of the chemical structure and on the concentration of the quencher [12]. The most active quenchers are organic acids, amines, alphaticalkens, sulphides, ketones, alphatic hydrocarbons and dissolved oxygen [9].

Colour quenching is caused by the attenuation of photons emitted by the scintillator. This is due to the presence of coloured substances in the radioactive solution or scintillator degradation. Colour quenching leads to anisotrophy of light emitted, which may cause problems in coincidence counting [1].

Ionization quenching is as a result of high ionization density along the track of a charged particle in the scintillator. The light emission L(E), produced by a charged particle interacting with the liquid scintillator is a non-linear function of particle energy, E. The non-linearity increases with the power of the particle and for example, a low-energy electron will cause higher ionization quenching than a higher energy beta particles [10].

1.3 Liquid Scintillation Counter

A scintillation counter measures ionizing radiation. The sensor called a scintillator consists of a transparent crystal, usually phosphor, plastic(usually containing anthracene) or organic liquid that fluoresce when struck by ionizing radiation. A sensitive photomultiplier tubes (PMT) measures the light from the crystal. The PMT is attached to the electronic amplifier and other electronic equipment to count and possibly quantify the amplitudes of the signals produced by the photomultiplier [3].

When a charged particle strikes the scintillator, a flash of light produced which may or may not be in the visible region of the spectrum. Each charged particle produces a flash. The association of a scintillator and photomultiplier with the counter circuits forms the basis of the scintillation counter apparatus. A charged particle passes through the phosphor, some of the phosphor`s atoms get excited and emit photons. The intensity of the light flash depends on the energy of the charged particles. Cesium iodide (CsI) in crystalline form is used as scintilator for the detection of protons and alpha particles. Sodium iodide (NaI) containing a small amount of thallium is used as a scintillator for the detection of gamma waves [13].

The scintillation counter has a layer of phosphor cemented in one of the ends of the photomultiplier, It`s inner surface is coated with a photo-emitter with less work potential. This photoelectric emitter is called as photocathode and is connected to the negative terminal of a high tension battery. A number of electrodes called dynodes are arranged in the tube at increasing positive potential when a charged particle strike the phosphor, a photon is emitted. This photon strikes the photocathode in the photomultiplier, releasing an electron. This electron accelerates towards the first dynode and hits it. Multiple secondary electrons are emitted, which accelerates towards the second dynode. More electrons are emitted, and the chain continues, multiplying the effect of the first charged particle. By the time the electrons reach the last dynode, enough have been released to send a voltage pulse across the external resistors. This voltage pulse is amplified and recorded by the electronic counter [3].

Scintillators , often converts a single photon of energy resolution into high number of lower energy photons, where the number of photons per mega electronvolt of input energy is fairly constant [14].

By measuring the intensity of the flash (the number of the photons produced by X-ray or gamma photon.), it is therefore possible to discern the original photon energy.

The sample to be analyzed has to be placed in direct contact with the scintillation medium liquid or solid, either by dissolving it into scintillation molecules of the medium or attaching it to a scintillation particle using some special binding reactions. In this interaction process most of the kinetic energy of the interacting beta particle is absorbed to the scintillator or solute that emits scintillation photons, whose amount is proportional to the energy of the interacted beta particle [14].

These scintillation photons are detected usually by photomultiplier tubes working in coincidence, which convert the photons into electric pulses. The coincidence method eliminates the thermal noise of the photomultiplier tubes. The heights of the pulses from the sample are proportional to the amount of the emitted scintillation photons and thus proportional to the energy of the interacted beta particle. Normally, the pulses from both the photomultiplier tubes are summed together [15].

A continuous spectrum corresponding to the energy distribution of the emitted beta particles is obtained by means of the multichannel analyzer incorporated in the counter, because the energies of the emitted beta particles are distributed in a way characteristic to the beta decay of the isotope to be counted [14].

This continuous spectrum has certain characteristic properties e.g. total counts, number of counts in a certain counting window or channel range of the multichannel analyzer, end point, maximum value and centre of mass, i.e. the centroid of the obtained spectrum. The channel of the multichannel analyzer can be calculated, in which the end point, the maximum value and the centre of the mass are located i.e. the channel co-ordinates of these values can be determined. The channel co-ordinates of the centre of mass of the spectrum is generally used as a measure of the quench level of the sample.

The counting efficiency of a liquid scintillation counter means the efficiency of the counting system to detect the beta particles emitted by the sample to be analyzed.

When measuring sample activities with liquid scintillation counters, a basic problem is the reduction in counting efficiency due to the quenching in the sample [4].

Because the quenching reduces scintillation photons, the spectrum also shifts to lower channels of the multichannel analyzer. Therefore an appropriate numerical factor describing the position of the spectrum e.g. the end point, maximum point or the centre of mass can be used as a quenching parameter. It is known that in liquid scintillation counting the reduction in the counting efficiency due to the quenching of the sample can be corrected by the use of a quench curve that describes the relationship between the counting efficiency and the amount of quench in the sample. The problem has been that the quench curves for chemically quenched and color quenched samples have not been exactly equal [4].

1.4   Aim and Objectives

The aim of this project is to use a Monte Carlo simulation code (GEANT4) to simulate the energy deposited by decay into the scintillation cocktail (the light output generated into the scintillation cocktail) using vials of sizes 10ml and 20ml containing a toluene solvent as the scintillator for ^{55}Fe and use a computer program VIASKL in computing the liquid scintillation counting efficiency.

The objectives of this work are;

- To use a computer simulation method GEANT4 in the computation of the photon scintillator interaction probability and energy spectrum (energy deposited by decay into scintillation cocktail or the light output generated into the scintillator) of ^{55}Fe using Toluene as the scintillator with different types of vial sizes.
- To use the result of the simulated data in the computation of the liquid scintillation counting efficiency by using the computer program VIASKL.
- To compare the counting efficiency with other reported efficiencies.

2.0   Literature Review

The chemical properties of an element are determined by its atomic number, the number of protons in the nucleus (and electrons within neutral atoms of that element). Uncharged neutrons, within the nucleus along with protons do not contribute to the atomic number, but will alter the atomic mass. This makes possible the existence of the Isotopes, which are atoms of the same element with different atomic weight. Most Isotopes are stable, and do not undergo any spontaneous nuclear changes. A subset of isotopes posses too few or too many neutrons to be stable. These are radioactive

atoms spontaneously rearrange their nuclei, emitting energy or particles in the process. [16].

Radioactive isotopes of common elements are extremely useful in life science disciplines, radioactive atoms can be substituted for their non-radioactive counterparts in chemical formulations. The resulting radioactive compound is easily detectable but still chemically identical to the original material. Two detection methods predominate for assaying such incorporated radioactivity. In autoradiography, labeled material is allowed to expose a photographic emulsion. Development of the emulsion reveals the distribution of labeled material. In the second detection method, the amount of radioactivity in labeled samples is directly measured either by a Geiger counter or by a scintillation counter. In scintillation counting the sample is mixed with a material that will fluoresce upon interaction with a particle emitted by radioactive decay. The scintillation counter quantifies the resulting flashes of light. [11].

2.1   Measurement of Radiation and Isotope Quantization

Most research applications of radioisotopes, at some stage, require quantization of the isotope, which is done by measuring the intensity of radiations emitted. Common nomenclature expresses this intensity as disintegrations per minute (DPM). The S.I. unit for radiation, the Becquerel (Bq), corresponds to 60 DPM [16].

Truly accurate measurement of DPM would require that every emission event be detected and counted, which is not possible in most situations. Additionally, naturally occurring isotopes and cosmic radiation contribute significant "background" radiations. Corrections for efficiency and background are needed to convert the counts per minute (CPM) measured into DPM, the number of decay events which actually occurred. Techniques have been developed for applying these corrections and a great deal of research has been carried out to improve the efficiency of counting using various detection systems [17].

2.1.1   Ionization Detection

Alpha, beta and gamma radiation all fall into the category of ionizing radiation. Alpha and beta particles directly ionize the atoms with which they interact, adding or removing electrons. Gamma-rays cause secondary electron emissions, which then ionize other atoms. The ionized particles left in the wake of a ray or particle can be detected as increasing conductivity in an otherwise insulating gas, which is done in electroscopes, ionization chambers or proportional counting chambers [18].

These devices measure the pulse of conductivity between two electrodes when a particle or ray ionizes the gas between them. If a sufficiently high voltage is applied between the electrodes, an amplification of the signal can be obtained, and such counters can be quite sensitive. Their utility is severely limited by the fact that for most research applications only gas phase isotopes can be detected. This greatly complicates sample preparation and may produce the analysis of some compounds entirely [19].

2.1.2   Scintillation detection

Some irradiated atoms are not fully ionized by collision with particles, but instead have electrons promoted to an excited state. Excited atoms can return to ground state by releasing energy, in some cases as a photon of light. Scintillation phenomena form the basis of a set of very sensitive radiation detection systems. In solid scintillation systems a crystal of inorganic or organic material, the scintillator is irradiated by the sample. The light emitted in response to this irradiation is taken as a measure of the amount of radioactivity in the sample. Solid scintillation is excellent for γ-radiation which is highly penetrating and can cause scintillation throughout a large crystal. An advantage of these techniques is that the same crystal is used for each sample, which enhances reproducibility. Unlike ionization counting a gas phase sample is not required. For α or β counting however, solid scintillation has severe limitations. The crystal must be protected from contamination by the sample, which means that the α and β-particles must traverse a barrier prior to reaching the scintillator. α–rays in particular are severely attenuated by even 0.05mm of aluminum or copper, and so cannot be expected to reach a scintillator crystal through even the thinnest shielding [20].

2.2   Mechanism of Liquid Scintillation Counting

By eliminating the combustion steps needed for gas phase analysis, the introduction of liquid scintillation counting (LSC) reduced the time required to analyze radioactive samples from hours to minutes. For low energy ("soft") β-emitters, LSC offers unmatched convenience and sensitivity. LSC detects radioactivity via the same type of light emission events which

are used in solid scintillation. The key difference is that in LSC, the scintillation takes place in a solution of scintillator, rather than in a solid crystal. This allows close contact between the isotope atoms and the scintillator, which is not an obstacle to detection [21].

Liquid scintillation cocktails absorb the energy emitted by radioisotopes and re-emit it as flashes of light. To accomplish these two actions, absorption and re-emission, cocktails contain two basic components, the solvent and the phosphor(s). The solvent carries out the bulk of the energy absorption. Dissolved in the solvent molecules of phosphor, convert the absorbed energy into light. Many cocktails contain additional materials to extend their range of use to different sample compositions, but the solvent and the phosphor provide the scintillation of the mixture [17].

2.2.1   The Role of the Solvent

The solvent portion of an LSC cocktail comprises from 60-99% of the total solution when a radioisotope dissolved in the cocktail under goes an emission event, it is highly probable that the particle or ray will encounter only solvent molecules before its energy is spent. For this reasons the solvent must act as an efficient collector of energy, and it must conduct the energy to the phosphor molecules instead of dissipating the energy by some other mechanism. The solvent must not quench the scintillation of the phosphor to produce a stable, countable solution [10].

2.2.2   The Role of Phosphors (Scintillators)

Phosphors are broadly divided into two classes primary and secondary scintillators. Included at 0.3-1% of the solution volume, primary scintillators provide the conversion of captured energy to the emission of light. The molecules of scintillator appear to induce a dipole moment in their salvation shell, allowing direct transfer of energy between the scintillator and excited solvent molecules separated by up to 10 other solvent molecules. Primary scintillators must be capable of being excited to a light emitting state by excited solvent molecules and they must be soluble in the solvent at a sufficient concentration to give efficient energy capture [15].

Secondary scintillators, or wavelength shifters, were originally included in scintillation cocktails to compensate for the narrow spectral response of early photomultiplier tubes. Most primary scintillators emit light below 408nm, but the response of early photomultiplier tubes drops significantly in this range. A secondary scintillator captures the fluorescence energy of the excited primary scintillator, and re-emits it as a longer wavelength signal. The process by which energy exchange takes place is not clear. (Although the emission spectrum of a primary scintillator and the absorption spectrum of the secondary scintillator generally over lap. The kinetics of the exchange suggests direct contact rather than an emission absorption event.

While modern phototubes are generally capable of counting the light pulses from the primary scintillator, secondary scintillators have been found to improve efficiency in many cases and are still included in most cocktails. It has been found that linked benzene rings, rather than larger aromatic systems, generally make superior scintillators [20].

2.30   Liquid Scintillation Signal Interpretation
2.3.1   Patterns of light emission

A β-particle passing through a scintillation cocktail leaves a trail of energized solvent molecules. These excited solvent molecules transfer their energy to scintillator molecules which give off light. Each scintillator molecule gives off only one photon on activation, (and the wavelength of that photon is characteristic of the scintillator, not the β- particle), but multiple scintillators are activated by the energized molecules generated by one β-particle. The path of a β-particle in a cocktail is generally less than 0.1cm; and the half-life is correspondingly short, which means that the burst of photons from an emission event derives from a small space and reaches the PMT with sufficient simultaneity to be read as one pulse of light. The number of photons generated is directly proportional to the path length of the β-particle, which is in turn determined by its emission energy (the β-particle rebounds from solvent molecule to solvent molecule) until its incident energy, is exhausted. The intensity of each light pulses per second corresponds to the emission energy and the number of pulses per second corresponds to the number of radioactive emissions [22].

2.3.2   Pulse Analysis

The scintillator counter classifies each pulse of photons according to the number of photons in the pulse, which corresponds to the energy of the individual β-emissions event. Pulses are collated into channels, and the count per minute(CPM) in each channel corresponds to a specific range of β-energies(channels are also known as counting

windows) and counts with energies above or below set limits are excluded from a particular channel. The usual practice is for three channels to be selected, which divide the energy spectrum of emissions into low, medium and high energy. The lowest channel corresponds to the energy of ^{3}H emissions, the highest to ^{32}P.

When the counts have all been collated, the researcher knows the intensity of radiation, expressed as CPM and its energy distribution, or spectrum. CPM is proportional to the amount of isotope in the sample, and the spectrum indicates the identity of the isotope. Within a theoretically ideal cocktail, all of the energy from each β-particle would be collected and converted into light. The spectrum of emitted energy and the DPM values could then be taken directly from the data. The highest energy emissions would be compared with the E-max (maximum emission energies) for known radioisotopes to confirm the isotope identity. Real cocktails, however, are less than 100% efficient in energy collection and conversion, especially with lower energy β-emission. This makes data interpretation somewhat more complex.

2.3.3   Counting Efficiency

While the effectiveness of a scintillation cocktail may be expressed a number of ways, it is most often given as percentage of emission events that produce a detectable pulse of photons referred to as the counting efficiency. In other words, counting efficiency is equal to

$$CPM/DPM \qquad\qquad (2.00)$$

The ratio of counts per minute (CPM) to disintegration per minute (DPM) is expressed as a percentage. Counting efficiency varies for different isotopes, sample compositions and scintillation counters. Poor counting efficiency can be caused by an extremely low energy to light conversion rate, (scintillation efficiency which even optimally, will be a small value. It has been calculated that only some 4% of the energy from a β-emission event is converted to light by even the most efficient scintillation cocktails. Fortunately, this number does not vary greatly across a wide range of β-energies, which avoids an additional level of complexity in signal interpretation [10].

However, the low efficiency in energy conversion means that low energy particles will only generate a few photons. Most phototubes used in scintillation detection only detect 1 in 4 photons so the average ^{3}H emission event will produce only a 20-25 photon pulse in the counter.

Clearly many emissions of below average energy or emissions which lose photons due to sample characteristics will fall below the level of a 1 photon event and will not register as a count on the instrument. The loss of CPM due to absorption of energy or photons by sample components is known as quenching. Quenching can easily reduce pulses below the detection limit of the counter, thus reducing the overall counting efficiency. The total counting efficiency for a detection system composed of two phototubes with the same gain, working in coincidence is: [23]

$$\in (M) = \ \sum_{n}^{N} Wn[\ I - \exp\ (\text{-En/2M})]^2 \qquad (2.01)$$

Where, n = 1----N.

And,

N – Is the number of different rearrangement pathways following the EC decay

W_n – Is the probability of the nth pathway

E_n – Is the effective energy of the nth pathway

M – Is the figure of merit

2.3.4   Quenching

Quenching is the loss of counts due to sample or cocktail characteristics and may result from a variety of components in a sample quenchers are or constantly divided into the categories of chemical quencher or color quenchers. Chemical quenchers absorb radioactive energy before it is converted to light. Therefore, chemical quenchers reduce the number of photons generated by each particle. Color quenchers absorb light in the range of the wavelength emitted by the scintillated by the scintillator. In this case, the number of photons emitted is not changed, but the number reaching the photomultiplier tube is reduced. Below this energy, particles do not generate enough photons to be detected [22].

In both types of quenching, the energy of all light pulses is reduced by the number of pulses quenched to below detectable levels. This leads to an underestimate of the total counts and thus of the isotope present. Also leads to an apparent shift in the energy spectrum of the sample [24].

2.3.5   Quench Correction

Various methods are available for quench correction. The most straight forward, but most laborious is the use of an

internal standard. A known amount of radioactivity, added to an unknown sample, will increase the DPM by a predictable amount. The difference between the increase in DPM observed and that expected is due to quenching and allows the determination of counting efficiency for that sample. The drawback to the use of internal standards is that each sample must be counted twice [25].It is also convenient to add an internal standard to many vials. Many scintillation counters offer the use of an external standard to correct for quenching [21].The number of photons generated is directly proportional to the path length of the β- particle, which is in turn determined by its emission energy (the β-particle rebounds from solvent molecule to solvent molecule, until its incident energy is exhausted. The intensity of each light pulse corresponds to the emission energy and the number of pulses per second corresponds to the number of radioactive emissions [26].

Birks, expressed the specific fluorescence $\frac{dL}{dx}$, the number of photons emitted per unit distance along the path, by a semi empirical formula:

$$\frac{dl}{dx} = \frac{n_o \frac{dE}{dx}}{1 + KB\left(\frac{dE}{dx}\right)} \tag{2.02}$$

Where n_0 is the scintillation efficiency or figure of merit (number of fluorescence photons emitted per unit of energy).

$\frac{dE}{dx}$ Is the stopping power of the incident particle and K is the ionization quenching parameter (Birks parameter) in units of gMeVcm-1. B(dE/dx) is the linear ionization density.

The fluorescent yield of the scintillator is given by:

$$L(E) = n_o \int_0^E \frac{dE}{1 + KB\left(\frac{dE}{dx}\right)} = n_o\, E Q\,(E) \tag{2.03}$$

Where Q(E) is the ionization quenching function.

$$Q(E) = \frac{1}{E} \int_0^E \frac{dE}{1 + KB\left(\frac{dE}{dx}\right)} \tag{2.04}$$

The computation of the ionization quench function presents three problems, the selection of the optimal value for KB, the stopping power value of energies lower than 1KeV and the composition of the commercial liquid scintillator, which atomic composition is not supplied by the firms [27].

2.4   Electron Capture

A nucleus can relieve a low neutron- proton ratio by capturing and absorbing an electron from a shell. Since most electrons are captured from the K shell, this process is sometimes referred to as K-capture. Capture from the L and M shells is possible under some conditions, but does not occur so frequently as from the K shell. When the negative electron enters the nucleus, the positive charge of one proton is cancelled and the proton is converted into a neutron. This results in the reduction of the atomic number by one unit. Since the mass number does not change, electron capture is an isobaric transition. Electron capture often competes with positron emission; if a nuclide is a positron emitter, some nuclei will emit positrons and some will capture electrons. The ratio between the two processes is specific for each nuclide [28].

In an electron capture transition, radiation is not emitted directly from the nucleus but results from changes within the electron shells. Electron capture creates a vacancy in one shell, which is quickly filled by an electron from a higher energy location. As the electron moves down to the K- shell, it gives off an amount of energy equivalent to the difference in the binding energy of the two levels. This energy is emitted from the atom in either characteristic X-ray photon or Auger electrons. Auger electrons are produced when the energy given up the electron filling the K-shell vacancy is transferred to another electron, knocking it out of its shell. Most Auger electron has relatively low energies [28].

2.5   Auger Effect

This is a physical phenomenon in which the transition of an electron in an atom filling an inner-shell vacancy causes the emission of another electron [29].When a core electron is removed, leaving a vacancy, an electron from a higher energy level may fall into the vacancy, resulting in a release of energy. Although sometimes this energy is released in the form of an emitted photon, the energy can also be transferred to another electron, which is ejected from the atom. This second ejected electron is called an Auger electron. The Auger emission process was discovered in 1922 by Lise Meitner, an Austrian physicist, as a side effect in her competitive search for the nuclear beta electrons with the British physicist Charles Drummond Ellis [30]. The French physicist Pierre Victor Auger also discovered it in 1923 [30].Upon analysis of a Wilson cloud chamber experiment. High energy X-rays were applied to ionize gas particles and observe photoelectric electrons. Observation of electron tracks independent of the frequency of the incident photon suggested a mechanism for

electron ionization that was caused from an internal conversion of energy from a radiationless transition. Further investigation and theoretical work showed that the effect was a radiationless effect more than an internal conversion effect by use of elementary quantum mechanics, transition rate and transition probability calculations [24].

2.6   Rearrangement Probabilities

Assuming, that electron capture is effective only on K and L shells and neglecting the L-subshells, there are 21 atomic rearrangement pathways: 18 of them correspond to interaction events and only three results in a total-energy escape. The probability of each pathway is given below;

If the rearrangement only involves Auger electrons, the probability is:

$W_1 = P_K a_K P_{KLL} a^2_L$ (2.05)

Where P_k is the probability for K electron – capture, a_k and a_L are the K and L-Auger yields and P_{KLL} is the fraction of the K-Auger emissions, corresponding to the KLL transition.

The coincident detection of two Auger electrons and just one X-ray can follow two different ways whose probabilities are:

$W_2 = 2P_K a_k p_{KLL} a_L w_L I_L$ (2.06)

$W_3 = 2P_K a_K P_{KLL} a_L w_L (1-I_L)$ (2.07)

Where w_L is the mean L-flourescense (figure of merit) yield and I_L is the escape probability for the X-rays from the transition LM.

The coincident detection of one Auger electron and two X-rays can be produced in three different ways:-

$W_4 = P_K a_K P_{KLL} w^2_L I^2$ (2.08)

$W_5 = P_K a_K P_{KLL} w^2_L (I – I_L) I_L$ (2.09)

$W_6 = P_K a_K P_{KLL} w^2_L (I – I_L)^2$ (2.10)

The emission of one LMM – Auger electron and one KL-X-ray can be detected in two ways,

$W_7 = P_K w_K P_{KL} a_L I_L$ (2.11)

$W_8 = P_K W_K P_{KLL}(1-I_K)$ (2.12)

Where W_K is the K-fluorescence yield, I_K and P_{KL} are the escape probability and the fraction of the K-X-ray emission corresponding to the KL-X-rays.

The coincident detection of just two X-rays gives the following probabilities:-

$W_9 = P_K w_K P_{KL} w_L I_K I_L$ (2.13)

$W_{10} = P_K w_K P_{KL} w_L (1- I_K) I$ (2.14)

$W_{11} – P_K w_K P_{KL} w_L (1-I_{IK}) (1 – I_L)$ (2.15)

$W_{12} = P_K w_K P_{KL} w_L (1-I_L) I_K$ (2.16)

The coincident detection of just two Auger electrons can be produced in only one way:

$W_{13} = P_K a_K P_{KLM} a_L$ (2.17)

The detection probability for one KLM –Auger electron and one LM – X-ray is given by:

$W_{14} = P_K a_K P_{KLM} w_L I_L$ (2.18)

$W_{15} = P_K a_K P_{KLM} w_L I_L$ (2.19)

The detection probability for one KMM – Auger emission can be obtained by:-

$W_{16} = P_K a_K P_{KLM}$ (2.20)

And for KM - X-ray:

$W_{17} = P_K w_K P_{KM} I'_K$ (2.21)

$W_{18} = P_K w_K P_{KM} (1 – I'K)$ (2.22)

$W_{19} = P_L w_L I_L$ (2.23)

$W_{20} = P_L w_L (1 - I_L)$ (2.24)

Where P_{KM} is the fraction of K-X-rays corresponding to the KM -transition and I'_K is the escape probability for the KM-X-rays.

Finally, the probability of emitting just one LMM- Auger electron is:

$W_{21} = P_L a_L$ (2.25)

Obviously, the following normalization constraints hold: [9].

$P_{KLL} + P_{KLM} + P_{KMM} = 1$ (2.26a)

$P_{LMM} = 1$ (2.26b)

$P_{KL} + P_{KM} = 1$ (2.27a)

$P_{LM} = 1$ (2.27b)

2.7 Pathways Effective Energies

The non-linear response of the scintillation system requires us to correct the total energy involved in each pathway by the ionization quenching function, giving the effective energy associated with that pathway from the point of view of the detection process [10].

The effective energies are:-

$E_1 = E_{KLL}Q(E_{KLL}) + 2 E_{LMM} Q (E_{LMM})$ (2.28)

$E_2 = E_{KLL} Q (E_{KLL}) + E_{LMM} Q (E_{LMM})$ (2.29)

$E_3 = E_{KLL} Q (E_{KLL}) + E_{LMM}Q(E_{LMM}) + E_{LM} Q (E_{LM}) + E_C Q (E_C)$ (2.30)

$E_4 = E_{KLL} Q (E_{KLL})$ (2.31)

$E_5 = E_{KLL} Q (E_{KLL}) + E_{LM} Q (E_{LM}) + 2 E_C Q (E_C)$ (2.32)

$E_6 = E_{KLL} Q (E_{KLL}) + 2 E_{LMM} Q (E_{LMM}) + 2 E_C Q (E_C)$ (2.33)

$E_7 = E_{LMM} Q (E_{LMM})$ (2.34)

$E_8 = E_{LMM} Q (E_{LMM}) + E_{KL} Q (E_{KL}) + E_C Q (E_C)$ (2.35)

$E_9 = 0$ (2.36)

$E_{10} = E_{KL} Q (E_{KL}) + E_C Q (E_C)$ (2.37)

$E_{11} = 2 E_{KL} Q (E_{KL}) + 2 E_C Q (E_C)$ (2.38)

$E_{12} = E_{KL} Q (E_{KL}) + E_C Q(E_C)$ (2.39)

$E_{13} = E_{KLL}Q(E_{KLL}) + E_{LMM}Q (E_{LMM})$ (2.40)

$E_{14} = E_{KLM} Q(E_{KLM})$ (2.41)

$E_{15} = E_{KLM} Q (E_{KLM}) + E_{LM} Q (E_{LM}) + E_CQ(E_C)$ (2.42)

$E_{16} = E_{KMM}Q(E_{KMM})$ (2.43)

$E_{17} = 0$ (2.44)

$E_{18} = E_{KM} Q(E_{KM})$ (2.45)

$E_{19} = 0$ (2.46)

$E_{20} = E_{LM}Q (E_{LM}) + E_CQ (E_C)$ (2.47)

$E_{21} = E_{LMM}Q (E_{LMM})$ (2.48)

Where E_{KLL}, E_{KLM} and E_{KMM} are the KLL – KLM – and KMM– Auger energies; E_{KL}, E_{KM} and E_{LM} are the KL–KM- and LM- X-ray energies when the binding energy for the K-electron in carbon is substracted, E_C is the KX-ray energy for carbon and finally ,Q(E) is the correction factor due to ionization quench.

A good approximation to Q(E) computed with recent values of dE/dx and taking KB=0.0075 cm/MeV is given by: [31].

$$Q(E) = \frac{A + B \, Log (E) + C \, Log^2 (E)}{I + D \, Log (E) + F \, log^2 (E)} \qquad (2.49)$$

Where: A, B, C, D, and F are constants given by;
A = 0.357478,   B=0.459577   C= 0.1599905, D = 0.0977557, F=0.215882 and Log (E) is the decimal algorithm of the energy [31].

3.0 Methodology

Different methods have been proposed for quantitative LSC measurement:the CIEMAT/NISTmethod [32]. and the triple-to-double coincidence ratio(TDCR) method [33]. Both methods need critical data in order to determine accurately the activity of the standards. Calculation of the counting efficiency for a specific nuclide and LS counter, together with the computation of the energy spectrum transferred to the liquid scintillator, becomes essential to the standardization methods. Several models[34; 35]. and computer codes [36;37]. have been used to calculate those data. To compute the LSC efficiency, the interaction probability and the Compton spectrum distribution must be obtained.

In this work, the Monte Carlo (MC) technique, using the GEANT4 toolkit [38]., in liquid scintillation counting (LSC) was applied, emission point of the photon is drawn according to the vial dimensions. The MC simulation includes a number of processes, namely, beta-ray generation, energy deposition into the scintillation cocktail, light production, light attenuation, photoelectron generation, and signal amplification in 2 photomultiplier tubes (PMT) working in coincidence. The simulation is carried out in such a way that several parameters can be calculated for a nuclide, like counting

efficiency, energy spectrum, or wall effects. The data used for the computation of the liquid scintillation counting efficiency was simulated using this computer simulation code GEANT4,which is a public software package composed of tools that can be used to accurately simulate the passage of particles through matter.

The MC simulations have been carried out through GEANT4 code.GEANT4 is a public toolkit for high-energy physics (HEP) experiments using an object-oriented environment and written in C++. GEANT4 is not only for HEP but also for cosmic rays physics, space science, and medical applications. In order to meet such requirements, a large degree of functionality and flexibility is provided for geometrical description, primary particle generation, physics processes, and visualization and analysis technologies [38].

The simulated setup includes a vial containing the scintillation cocktail in between two opposite photomultipliers tubes (PMTs) working in sum-coincidence mode. The decay of several beta emitters (such as ^{14}C and ^{3}H) can be simulated, as well as alpha or EC emitters. Additionally, significant information could be obtained, such as the energy deposited by decay into the scintillation cocktail or the light output generated into the scintillation cocktail. The sample to be analyzed is placed in direct contact with the scintillation medium liquid or solid. In this interaction process most of the kinetic energy of the interacting particle is absorbed to the scintillator which emits the scintillation photons, whose amount is proportional to the energy of the interacted particle. These scintillation photons are detected by the photomultiplier tubes. The heights of the pulses from the sample are proportional to the amount of emitted scintillation photons and thus proportional to the energy of the interacted particle. Normally, the pulses from both the photomultiplier tubes are summed together.

GEANT4 is a useful tool for efficiency calibration, stopping power calculations, or wall effect studies for different scintillation cocktails and geometries.

In GEANT4 code (version 8.2), highly complex setups and a rich set of solid types (simple solids, Boolean solids, BREPS [Boundary Represented Solids]) containingdifferent materials are available for describing the geometry setup of each experiment. Additionally, various utilities provided within the GEANT4 toolkit help for the generation of primaries particles in the simulation.GEANT4 allows the selection of particle type (all PDG data and even radioactive ions), energy, and momentum, together with its distribution into different areas or volumes. The GEANT4 toolkit includes the simulation of electromagnetic physical processes from 1 keV to100 TeV. The processes associated to gammas are the photoelectric effect, Compton scattering, pair production, and electron and muon pair production. For electrons and positrons, the processes included are ionization and delta ray production bremsstrahlung, e+e−annihilation, and synchrotron radiation. Finally, the physical processes corresponding to all charged particles are made up of multiple scattering, transition radiation, as well as scintillation and Cherenkov radiation. These last 3 processes are vitally important to simulate a LSC counter using the GEANT4 toolkit. If a charged particle produced in the decay of the radionuclide traverses a dielectric material with velocity above the Cherenkov threshold or a scintillating material, an optical photon is produced.

A photon is called optical when its wavelength is much greater than the typical atomic spacing. Next, the optical photons undergo 3 kinds of interactions: elastic (Rayleigh) scattering; absorption; and medium boundary interactions (refraction and reflection) along the geometry of the simulated setup. The simulated setup consists of a LS counter system (Quantulus1220TM) and WheatonTM borosilicate glass vial of 20 ml. The counter is made up basically of 2 PMTs (model HamamatsuTM R331-05) working in coincidence, and the materials and dimensions of the window and the photocathode are included into the simulation [39]. The simulated vial contains a standard of Fe55 into 10 ml of a toluene-based LS cocktail.

The result of the simulation computes the nuclide data for Fe55 and the photon-scintillator interaction probability data for Toluene using different vial sizes and radius.

The program VIASKL was used in the computation, it consist of a main program, 16 subprograms and two data files. The initial setting of the input-output (I/O units), input data specification : nuclide, scintillator, radius, volume, upper and lower bounds and increment for the figure of merit (FACTI, FACTF, DFACT), number of statistical samples (NHIS), assignment of default values to variables, and computing the efficiency and standard deviations of the NHIS samples, controls the overall flow of the program. It also includes implicit calls to subroutines that accomplish special tasks: nuclide and data input (RENUCL,RESCIN) from the data files VIASNUC, VIASSCI, respectively, X-ray photon scintillator interaction probability evaluation (PROINT,DAITIN,INDIN), probability and effective energy computations (PROVIA,ENVIA,EQ) for each of the 21 rearrangement path ways following the capture, random simulation (UNCER, DUPLI, LIGRAN, RANSET, FRANDU, FRANDN, FRANDE) of the NHIS additional data sets that take into account the uncertainties in the experimental parameters, and the printing of efficiency-figure of merit (WREFIT) [23]. The model

assumes a pure electron-capture nuclide it does not take into account more complex decay schemes with gamma transitions following the capture. The contributions of electron capture in M-shells or higher to the total counting efficiency is neglected.

The program VIASKL was used in the computation of the liquid scintillation counting efficiency of ^{55}Fe (a K-L-shell) electron radionuclide using different type of scintillator and vial sizes. It gave the efficiency for each figure of merit.

The output of the program gives the tables of energies and intensities for the Auger transitions (KLL, KLM, KMM, LMM) and for that of X-rays (KL, KM, LM) transitions for different nuclides and the result of the capture probabilities and Flourescense yield for both K and L capturing shells were obtained, the graph of the energy against the intensity for the auger and X-ray transitions were plotted. The output data for the computation of the efficiency against figure of merit for ^{55}Fe were obtained

Each efficiency calculation for a given nuclide and a given scintillator and vial size requires only one input data line, as described in Table 3.1.

Table 3.1: Description of input data line for program VIASKL

Line	Format	Variable name	Type	Meaning
1	Free	NUC	Character * 8	Name code of nuclide
		SCI	Character*8	Name code of scintillator
		VOL	REAL	Volume (in ml) of the Vial
		RADIUS	REAL	Radius (in cm) of the vial
		FACT I	REAL	Initial figure of merit
		FACT F	REAL	Final figure of merit
		DFACT	REAL	Increment for the figure of merit

3.1   Subroutine Renucl

In this subroutine, the experimental mean values of the atomic parameters of the nuclide that are needed for the calculation are read from the data file VIASNUCL: electron capture probabilities: P(K),P(L).Fluorescence yields: W(K),W(L). Auger transition probabilities: PA(KLL), PA(KLM), PA(KMM). Auger transition energies: E(KLL), E(KLM), E(KMM), E(LMM). X-ray transition probabilities: PX (KL), PX(KM). X-ray transition energies: EX(KL), EX(KM), EX(LM), as well as their respective standard deviations (in %). DP, DW, DPA, DEA, DPX, DEX.

3.2   Subroutine Rescin

In this subprogram, the interaction probabilities of photons with the specified scintillator at several selected energies of photons are read among those corresponding to different geometries of vials, from the data file VIASSCI to the variables: ET(n): nth energy in KeV, PT(n): interaction probability for photons of energy ET(n).DPT(n): standard deviation of PT(n), in %
 n=1,2,……,NE<100.

3.3   Subroutines Proint, Daitin, Indin

The subprogram PROINT computes the actual interaction probabilities of the X-ray photons emitted in the atomic rearrangement following the electron capture with the scintillator. To that aim, the pairs ET(n),PT(n) are interpolated at the X-ray energies EX(i, j) to produce the variables PIX(i, j).

An estimation of the uncertaintiy in PIX(i, j) is also obtained by interpolating the pairs ET(n), PT(n)-DPT(n) at the experimental upper bound of X-ray energies EX(i, j)+DEX(i,j), the result being stored in DPIX(i,j). In both cases, a second degree Aitken interpolation algorithm is used, calling the routines DAITIN, INDIN.

3.4   Subroutines Provia, Envia, EQ

 In these subprograms, the probabilities and effective energies of the 21 rearrangement pathways are evaluated as indicated in the theory and stored in the variables PROB(m), ENER(m)= 1,2,3,……..21, respectively. The function EQ(E)

performs the ionizing quenching correction of the energy E appearing as argument, multiplying E by the factor Q(E) given in the equations earlier in chapter two.

3.5   Subroutines Uncer, Dupli, Ranset, Frandn, Ligran, Frande, Frandu

The subroutine UNCER works in two different forms depending on the value of the variable NH. If NH= 1, the subroutine DUPLI is called to save the parameters of the nuclide and the scintillator into auxiliary variables, and the starting point of a machine independent uniform random numbers generator is set up by calling the routine RANSET. The control is transferred to the main program in order to carry out the computations of efficiency using the mean values of the parameters.

If NH=2, or higher, the routine FRANDN is called to draw a random estimate of each parameter, assuming a normal distribution with the original mean value and standard deviation saved in the first call to UNCER. Then, control is returned to the main program to go on the computations over the new simulated set of parameters.

Each time a parameter sample is obtained; several checks are made to reject meaningless situations like negative or greater than unity values of the individual probabilities or the fluorescence yields, or negative energies. The probability normalization constraints are granted by the subroutine LIGRAN.

The routine FRANDN includes calls to FRANDE, an exponential random number generator and both rest on FRANDU, the machine independent uniform random generator which will allow other users to reproduce the test results.

3.6   Subroutine Wrefit.

This subroutine prints out a table of the efficiency versus the figure versus figure of merit varying from FACTI, to FACTF in steps of DFACT. Depending on the value of its argument ITY, which is controlled by the main program, two kinds of tables are produced.

4.0   Results And Discussion
4.11   Simulation Results for Geant4

The result of the nuclide data simulated and the photon scintillator interaction probability data are presented in Tables 4.1 and 4.2 .

Table4.1: Simulated nuclide data for ^{55}Fe.

Transition	Energy(KeV)	Probability(%)	Standard deviations(%)
AUGER			
KLL	5.0800	0.8024	25
KLM	5.8000	0.1822	20
KMM	6.4500	0.0154	25
LMM	0.6200	0.0000	23
X-RAY			
KL	5.8900	0.8920	10
KM	6.4900	0.1080	10
LM	0.6400	0.0000	15

The interaction probabilities of photons with the specified scintillator at several selected energies of photons which will correspond to different geometries of vials are generated. ET(n) gives the nth energy in KeV, NV is the number of different volumes associated with the radius and V(n) in ml are the actual values of these volumes. Table 4.02 gives the simulated data for the photon-scintillator interaction probabilities.

Table 4.2: Photon-scintillator interaction data.

	NV(ml)	V(1)	V(2)	V(3)	V(4)	V(5)	V(6)	V(7)
	7	1	2	3	5	10	15	20
ET(n)	0.0000							
1	1.0000	0.9885	0.9991	0.9995	0.9995	0.9995	0.9996	0.9996
2	3.0000	0.9610	0.9784	0.9835	0.9877	0.9911	0.9922	0.9924
3	5.0000	0.8190	0.8937	0.9203	0.9404	0.9574	0.9696	0.9649
4	7.0000	0.5876	0.7240	0.7883	0.8397	0.8806	0.8958	0.9032
5	10.0000	0.3270	0.4563	0.5308	0.6161	0.6960	0.7260	0.7411
6	15.0000	0.1494	0.2218	0.2706	0.3365	0.4082	0.4445	0.4646
7	20.0000	0.0929	0.1395	0.1735	0.2171	0.2763	0.3077	0.3229
8	25.0000	0.0689	0.1093	0.1330	0.1681	0.2192	0.2438	0.2567
9	30.0000	0.0589	0.0952	0.1168	0.1476	0.1882	0.2130	0.2244
10	50.0000	0.0476	0.0737	0.0917	0.1184	0.1523	0.1718	0.1801
11	100.000	0.0390	0.0599	0.0752	0.0968	0.1246	0.1389	0.1487
12	200.000	0.0308	0.0460	0.0600	0.0782	0.1012	0.1137	0.1204
13	500.000	0.0227	0.0349	0.0437	0.0551	0.0739	0.0833	0.0894
14	800.000	0.0196	0.0296	0.0368	0.0471	0.0617	0.0696	0.0745
15	1000.00	0.0185	0.0270	0.0347	0.0444	0.0566	0.0646	0.0697

4.12   Results of Viaskl

The graphs of the radius of the vial against scintillator type (code) and the volume of the vial against the scintillator type (code) were plotted as cited in Figure. 4.1 and Figure.4.2. Graphs of capture probability against nuclide (codes) for K and L shells are plotted and cited in Figures 4.3 and 4.4.Graphs of the fluorescence yield against nuclide (codes) for the K and L shells were also plotted and cited in Figures 4.5 and 4.6. The intensity against energy graph for the Auger and X-ray transitions were also plotted and cited in Figures 4.7, 4.8, 4.9, 4.10, 4.11, 4.12, and 4.13.
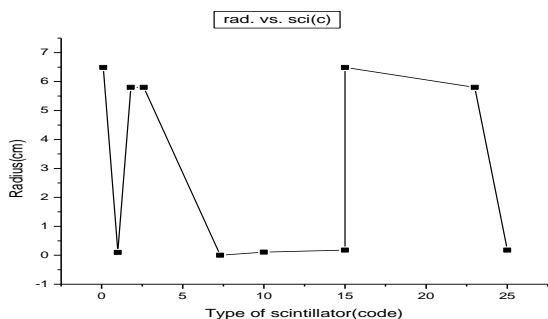
Fig.4.1: Graph of radius(cm) of the vial used against types of scintillators.
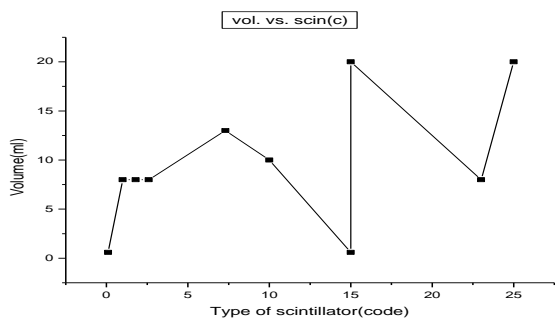
Fig.4.2: Graph of the volume(ml) of the vial against the type of scintillators used
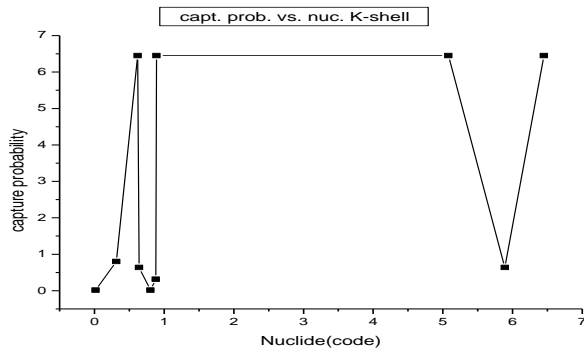
Fig.4.3: Graph of the capture probability against nuclide for a K-Capturing shell.
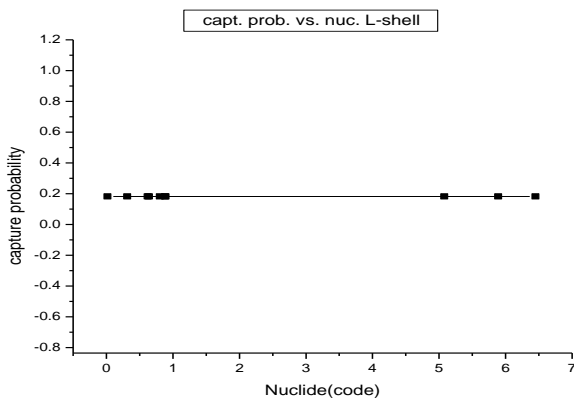
Fig.4.4: Graph of the capture probability against nuclide for an L-capturing shell.
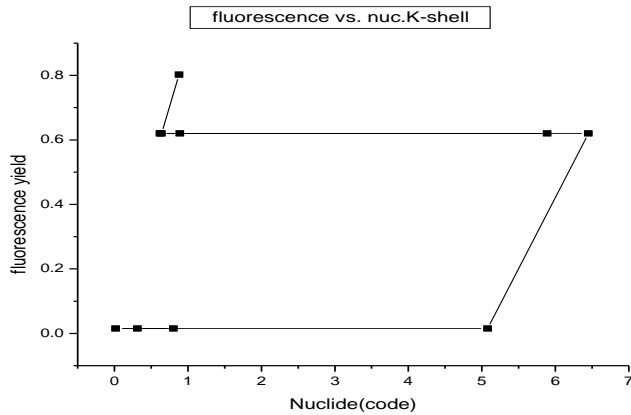
Fig.4.5: Graph of the flourescence yield against nuclide for a K-capturing shell.
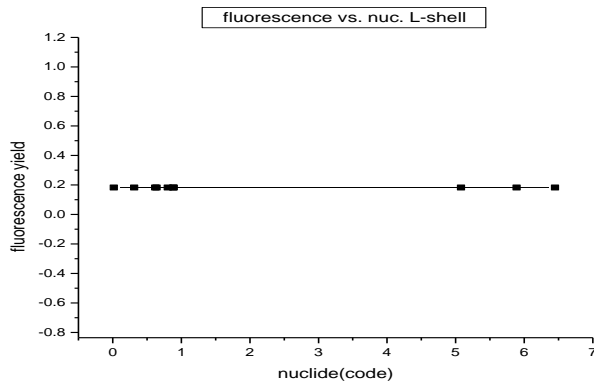
Fig.4.6: Graph of the flourescence yield against nuclide for an L-shell.
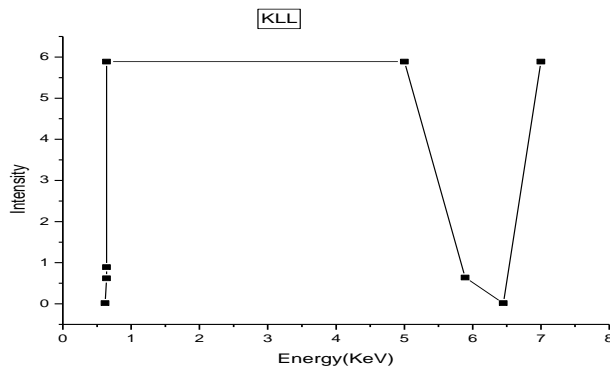
Fig.4.7: Graph of the intensity (cpm) against energy (KeV) for KLL-Auger transition.
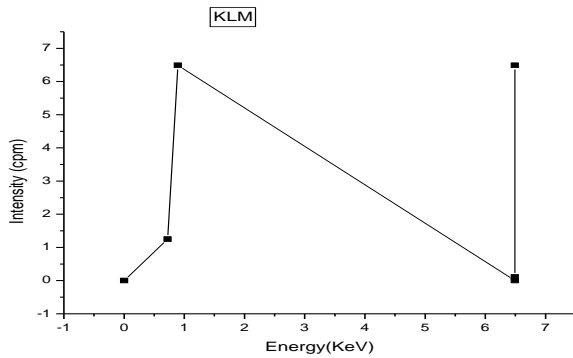
Fig.4.8: Graph of intensity(cpm) against energy(KeV) for KLM-Auger transition.
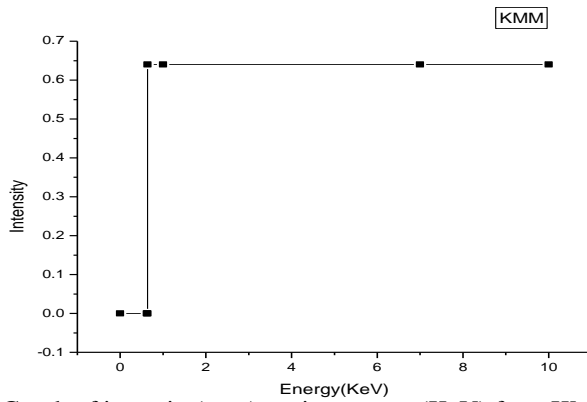
Fig. 4.9: Graph of intensity(cpm) against energy(KeV) for a KMM-Auger transition.
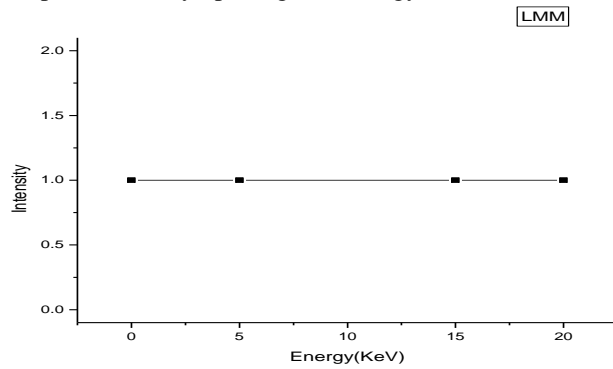
Fig. 4.10: Graph of intensity (cpm) against energy (KeV) for an LMM-shell transition.
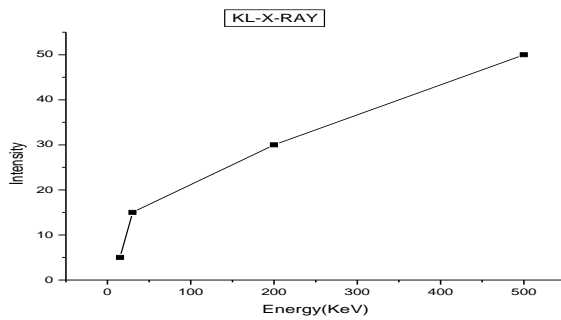
Fig. 4.11: Graph of intensity (cpm) against energy (KeV) for a KL-X-ray transition.
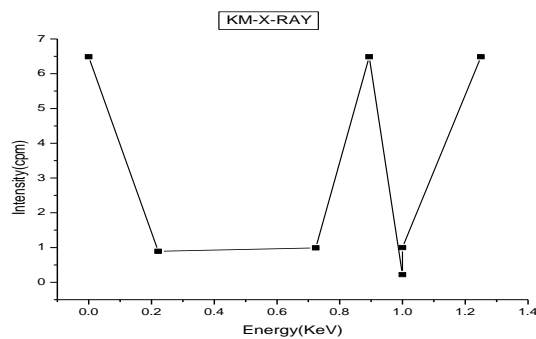
Fig. 4.12: Graph of intensity (cpm) against energy(KeV) for a KM-X-ray transition.
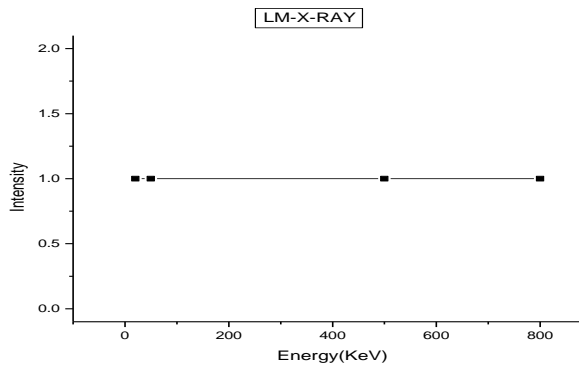
Fig. 4.13: Graph of intensity (cpm) against energy (KeV) for an LM-X-ray transition.
The graph of the liquid scintillation counting efficiency against figure of merit for ^{55}Fe was plotted and compared with that of ^{55}Fe (Fernandez,A.et.al.,1985). These graphs are cited in figures; 4.14 and 4.15 below.
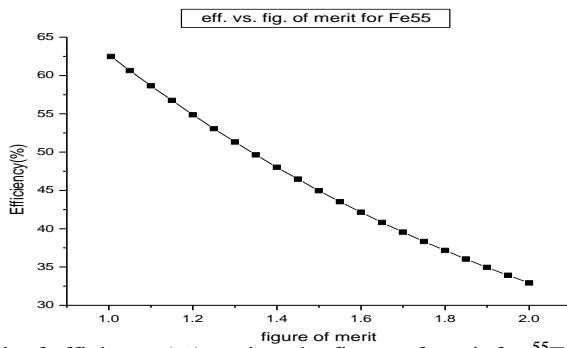
Fig.4.14: Graph of efficiency (%) against the figure of merit for ^{55}Fe (using VIASKL)
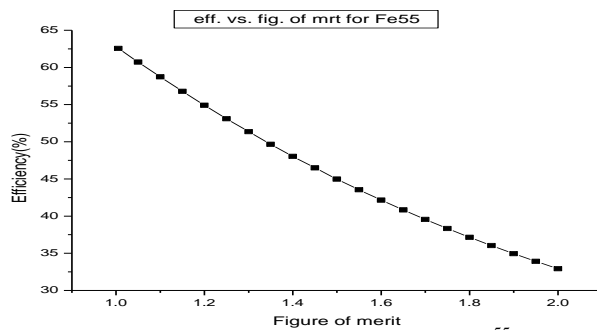
Fig. 4.15; Graph of efficiency(%) against figure of merit for ^{55}Fe (Fernandez, A.et.al.,1985).

4.2   Discussion

Fig.4.1Shows the graph of the variation of radius of the vial used with the type of scintillator. It shows that at a point where the radius is equal to 6.60cm the scintillator is equivalent to 0.00, the radius then decreases to a point of 0.11cm and the scintillator becomes 1.30 and then the radius increases to 5.79cm at a scintillator point of 1.90. At this radius the scintillator changes at a constant radius and the radius now decreases with change in scintillator to a point of 0.11cm. The scintillator now changes with a slight change in radius of the vial and then the radius again increases at a constant value of the scintillator to a point of 6.4cm. The radius of the vial now decreases at a change of scintillator and then decreases with another scintillator to a point of 0.19cm. This indicates that different scintillators can be used with the same radius of

the vial and or the different radius but the same scintillator (the radius of the vial can be varied with the same or different scintillator).

In Fig.4.2: The graph of the variation of volume with scintillator was plotted. This graph shows that at a volume of 0.21ml the scintillator point is equal to 0.01 the volume increases at this point to a value of 6.04ml with a change in the scintillator of 1.12. The volume becomes constant with various type of scintillators and the volume then increases with a change in the type of scintillator from point 6.04ml to 13.04ml, then the volume decreases slightly with a change of scintillator to a point of 10.0ml and scintillator point of 9.97, then increases to a point of 19.95ml and the scintillator changes to 15.0. At this scintillator type the volume decreases to 0.57ml and then increases to a point of 7.93ml and the scintillator also changes to 22.97. The volume then increases again to a maximum point of 20.ml with scintillator 24.97. This also shows that different scintillators can be used with different volume and or with the same volume of vial.

Fig.4.3: Shows the graph of capture probability against nuclide for the K-capturing shell. At nuclide value 0.0064, the capture probability equals approximately 0.0110, then the capture probability increases linearly with nuclide from 0.3270 to 0.7281.The capture probability increases linearly with the nuclide from this point to 6.4710. It then decreases linearly to a value of 0.0117 and a nuclide value of 0.7972. The capture probability then increases with constant value of the nuclide to a value of 5.092 and then decreases linearly with a nuclide value of 5.8690 to a value of 0.6258 and then the values increases linearly. This shows that the capture probability of a nuclide for the K-capturing shell is linearly independent with the type of nuclide.

Fig. 4.4: This graph shows the variation of the capture probability with the type of nuclide for the L-capturing shell. This shows that at a nuclide of 0.0202 the capture probability is equal to 0.1799. The capture probability remains constant as the type of the nuclide changes from a value of 0.3270, 0.63050, 0.77056, to 2.7914, 5.0600,5.8961,6.4230. This indicates that different nuclides possess the same capture probabilities in the L-shell.

Fig. 4.5: Is the graph of fluorescence yield against nuclide type for the K-capturing shell. At point 0.0469 of the nuclide, the fluorescence yield is equal to 0.0135. the nuclide changes at a constant capturing probability and then at a nuclide value of 5.039 the two values increased linearly to a point (6.4230,0.6210). then the value of the nuclide changes decreasingly with constant fluorescence to a nuclide value of 0.6305 and the two values increases linearly to points(0.8806,0.8028). With this graph it is shown that different nuclides can have the value of fluorescence yield.

Fig. 4.6. Is the graph of the fluorescence yield against nuclide for the L-shell. At a fluorescence yield point of 0.1799, the nuclides possess values of 0.0064, 0.5806, 5.065, 5.8961, 6.4530. This shows that for different nuclide the fluorescence yield for the L-shell is constant.

Fig. 4.7. Is the graph of intensity against energy for KLL-Auger transition. At a point where energy (E) equals to 0.6438KeV, the intensity (I) is equal to 0.04259cpm, I increases at this value of E up to I=5.911cpm, then E increases with constant I, at E= 5.01KeV, I decreases linearly up to a point where I becomes equal to 0.646cpm and E=5.90KeV it then converges linearly to a point where I=0.012cpm and E=6.498KeV, then E and I increases linearly. This shows that for KLL-Auger transition of various nuclides, the energy of the emitted electrons does not depend on the intensity of the incoming light, but only on the frequency of the individual photons.

Fig. 4.8. Is the graph of intensity against energy for KLM-auger transition. This shows that at a point where energy E=0.7189KeV the intensity I=1.1992cpm, at this point I and E increases linearly to a point (0.8995,6.4792) then the values decreases linearly to point (6.4895,0.0439) then the intensity I increases with constant energy to a value of 6.4792.. This graph also shows that for a KLM-Auger transition the energy of the emitted electrons depends on the energy or frequency of the individual photons.

Fig. 4.9. shows the graph of intensity against energy for a KMM-auger transition. For a KMM- auger transition the graph shows that at a point where E=0.0084KeV,

I=0.0017cpm, E increases at constant I up to E=0.67KeV, then I increases at constant E up to I=0.64cpm, and E then increases at constant I up to E=9.90KeV.

Fig. 4.10.This shows the graph of intensity against energy for LMM-auger transition. This graph shows that for nuclides of different energy, the intensity remains constant for an LMM-auger transition. At a point of I=1.00cpm, E=0.12KeV. At this constant value of I, E increases from 4.95KeV to 15.04KeV to 20.12KeV. Showing that for nuclides with different values of energy the intensity for the LMM-Auger transition the intensity is constant.

Fig. 4.11, is Graph of intensity against energy for KL-X-ray transitions. At a point where E=16.16KeV, I=5.25cpm and at this point I increases with a slight increase in E to a point where I=14.98cpm and E=31.63KeV then E increases linearly with I.

Fig. 4.12. Also shows the graph of intensity against energy for KM-X-ray transition.

In this graph at point (0.0012, 6.5087) I deceases linearly with E to a point (0.2201, 0.9287), then I increases linearly with E up to a point (0.7250, 0.9983). I increases linearly again with E to point (0.8911, 6.4718), it also decreases with E to a point (1.0018, 0.2164), and then increases again to a point (1.2572, 6.5087). This shows that as intensity increases, energy of the electron also increases.

Fig.4.13 is the graph of intensity against energy for an LM-X-ray transition. This graph also shows that for an LM-X-ray transition, the intensity of different nuclide with different energy is constant. At a point where the intensity is equal to 1.0cpm the value of energy equals 24.94KeV and the same value of I, energy E increases to a point of 50.93KeV, then increases to 494.041KeV, and then to a value of 804.85KeV. This shows that for nuclides of different energy the intensity for LM-X-ray emission remains constant.

In general this is in agreement with the photo emission process whereby if an electron within some material absorbs the energy of one photon and acquires more energy than the binding energy of the material, it is ejected. If the photon energy is too low, the electron is unable to escape the material. Increasing the intensity of the light increases the number of photons emitted, and thus increases the number of electrons excited, but does not increase the energy that each electron possesses. The energy of the emitted electrons does not depend on the intensity of the incoming light, but only on the energy or frequency of the individual photons. It is an interaction between the incident photon and the outermost electron. Electrons can absorb energy from photons when irradiated, but they usually follow an "all or nothing" principle. All of the energy from one photon must be absorbed and used to liberate one electron from atomic binding, or else the energy is re-emitted. If the photon energy is absorbed, some of the energy liberates the electron from the atom, and the rest contributes to the electron's kinetic energy as a free particle.

Fig.4.14. Shows the graph of efficiency against the figure of merit for ^{55}Fe (K-L-shell model). It shows the variation of efficiency with the fluorescence yield (figure of merit) in that at a point where the figure of merit is equal to 1.07 the efficiency is approximately equal to 62.50% and at a point where the figure of merit equals to 1.5 the efficiency is equivalent to 45.5%, the efficiency decreases with an increasing figure of merit (i.e. from 62.50% to 32.60% and 1.07 to 2.0).

The average efficiency and figure of merit for ^{55}Fe was calculated by taking some points from the data. The mean efficiency was calculated to be equal to 46.67% and the mean figure of merit was calculated to be 1.5064.

Fig.4.15, shows the graph of efficiency against figure of merit for ^{55}Fe (Fernandez, A.et.al.1985). At an efficiency of 62.5354% the figure of merit is equal to 1.0056 and at an efficiency of 48.1113% the figure of merit equals 1.3956. the efficiency decreases to 32.8657% with a figure of merit equal to 1.9991. These gave us a mean efficiency of 47.5354% and a mean figure of merit of 1.4679.

When compared with the efficiency computed, this shows that the values are almost similar and also as the efficiency decreases the figure of merit increases for both results.

5.0   Summary, Observations and Conclusion
5.1   Summary

Liquid scintillation counting efficiency (LSC) techniques can be used for radionuclide standardization when the calculation of detection efficiency is possible. These calculations are based on the statistical and physical models of the source and the detector and require the calculation of energy transferred to the scintillator, which is generally taken as the electron spectrum emitted by the measured nuclide (using a model of the physicochemical processes involved in light emission and also of the statistics of photon emission).

The program VIASKL was used in computing the liquid scintillation counting efficiency of the electron capture nuclides for different values of the figure of merit (which is the ratio between the deposited energy into the liquid scintillator by the interacting particle) using different types of scintillators and vial sizes. It was also used to compute the energy and intensity for both Auger(KLL,KLM,KMM, and LMM) and X-ray(KL,KM and LM) transitions because the computation of the counting efficiency requires also the determination of averaged energies for the considered Auger-electron emission. The result of the computations of the intensity and energy of the Auger and X-ray transitions were presented graphically and also the relationship of scintillator with the radius and volume of vial were determined and presented graphically. The mean efficiency was calculated from the graph to be equal to 46.6755% and the mean figure of merit to be equal to 1.5064.

5.2 Observations

Calculation of the detection efficiency in LSC relies on the correct evaluation of the energy spectrum transferred to the LS cocktail. The implicit assumption behind this is that the nuclide to be measured is the expected one. If the radioactive solution contains a non-negligible amount of impurities, the calculation model can be biased or the calculated spectrum must be modified accordingly. This means that, if the concentration of radioactive impurity is not negligible in terms of the expected uncertainty of measurement, qualitative and quantitative impurity evaluation is necessary.

The intrinsic resolution of LSC spectra is governed by the low light yield of the LS process, producing large statistical fluctuations of the number of photons emitted. The relative resolution depends on the intrinsic efficiency of the scintillator and also on the design of the optical chamber of the counter. The resolution is also much lower in the low-energy region and the spectra are not linear because of the ionization quenching phenomena. In this case, proper windows can be determined to allow rough quantitative impurity measurement.

Relative LSC activity measurements methods are proposed by commercial LS counter manufacturers. These methods are based on experimental or calculated efficiency versus quenching curves for each radionuclide measurements but if relative uncertainties of about 1% are needed, it is necessary to check that the measurements is made under the same conditions as the one used to obtain the efficiency curve. This includes the use of the same vial, the same volume of scintillator, the same LS cocktail from the same batch and the same aqueous content and chemistry of the radioactive solution. If these requirements are not fulfilled, bias of several per cent can be encountered, especially for low-energy radionuclides like ^{3}H, ^{55}Fe, e.t.c.

The number of radionuclide's standardized by LSC techniques is increasing with time and these methods are now used in most national radionuclide metrology laboratories. Some developments of quantitative LSC methods are still needed, concerning for example calculation of scintillator non-linearity or statistical description of the light emission, but LSC standardization methods have greatly matured and play an important role in radionuclide metrology.

5.3 Conclusion

The computer simulation method GEANT4 was used in the simulation of the energy deposited by decay into a scintillation cocktail for different scintillation cocktails and geometries and this data was used in the program VIASKL to compute the liquid scintillation counting efficiency for ^{55}Fe.This efficiency was approximately computed as 46.6755% and the figure of merit computed as 1.5064. This computed value was compared with a reported computed value of ^{55}Fe whose efficiency was computed to be approximately equal to 47.5354% with approximate figure of merit as 1.4679 [23]. The energy of the auger transitions was computed to be averagely equal to 220.3797KeV and the intensity computed to be averagely equal to 77.6042 counts per minute. The average energy for X-ray transition was also computed to be equal to 3711.477KeV, while the X-ray transition intensity was computed to be averagely equal to 265.5046 counts per minute.

6.0 Reference

[1]   Vatin, R., 1980 . The use of liquid scintillators in Radionuclide Metrology, BIPM monograph.

[2]   Ryzard,B. Cassette, P. Karsten, K., 2007. Radionuclide metrology using liquid scintillation counting . Institute of Atomic Energy. Radioisotope centre POLATOM, 05-400 Otwock-Swierk. Poland.

[3]   Wikipedia, the free encyclopedia:Retrieved from"http//en.wikipedia.org/wiki/Scintilation counter"

[4]   Lehtinen, I. Hannaher, H. Constantine, E.,1992. Method for the correction of an error caused by variations in the sample volume in a liquid scintillation counter. November, 22, 1994.

[5]   Dobrin, R. Dulana, C. Toma, A. Paunoiu, C., 2006. Study of the performance of the Efficiency Tracing Technique On A Tricarb2100TR Liquid Scintillation Analyzer. International Conference Nuclear Energy For New Europe, Portoroz, Slovenia, September 18-21, 2006.

[6]   Willard, G.W., 2004. Standardization of pure beta emitters by liquid scintillation counting. Applied radiations and isotopes, 39(2): 159-164

[7]   Cassette, P., 1992. Experimental evaluation of TDCR models for the 3-PMT Liquid scintillation counter. Nuclear, instrumentation methods of physics. 312, 95.

[8]   Broda R, Cassette P, Kossert K., 2007. Radionuclide metrology using liquid scintillation counting. Metrologia 44:36–52.

[9]   Broda, R. Maletka, K. Terlikowska, T. and Cassette, P., 2007. Study of the influence of the LS-Cocktail composition for the standardization of radionuclides using TDCR model. Applied radiation and isotope 56,285-9.

[10]   Birks, J.B., 1964. The theory and practice of scintillation counting. PergamonPress, Oxford, U.K.

[11]   Cassette, P. Broda, R. Hainos, D. and Terlikowska, T., 2000. Analysis of detection – efficiency variation techniques for the implementation of the TDCR method in Liquid scintillation counting. Applied Radiations and Isotopes. 52, 643-8.

[12]   Grau, M. and Grau, C.A.,1999. The ionization quench, factor in liquid scintillation counting standardizations. Applied Radiation and isotopes, 51, 183.

[13]   Knoll, Glenn. 1999. Radiation Detection and Measurement. J. Wiley and sons. ISBN -0-471-07338-5.

[14]   Schell, W.R. Mitchell, P.I., 1993. Optimization and Calibration of a Lowbackground Liquid Scintillation Counter for the simultaneous determination of alpha and beta emitters in aqueos samples. Liquid Scintillation Spectrometry,1992,edited by Noakes, J.E.,Schonhofer,F. Polach,H.A., Radiocarbon 1993,43-50.

[15]   Horrocks, D.L, Studier, M.H. 1961. Determination of the absolute disintegration rates of low energy beta emitters in a liquid scintillation spectrometer. Analytical Chemistry 33:615.IBJ Report INR 1848/OPiDi/E/A. Swierk, Poland.

[16]   National Diagnostics Laboratory Staff. Principles and Applications of Liquid Scintillation Counting. A primer for orientation.

[17]   Knoche, H.W., 1991. Radioisotopic Methods for Biological and Medical Research Oxford University Press, NY.

[18]   Schimel, David, S.,1993. Theory and Application of Tracers. Academic Press.

[19]   Coleman, David, C. and Brian, F. (eds), 1991. Carbon isotope techniques. Academic Press.

[20]   Wilkinson, D.H.,1950. Ionization Chambers and Counters. Cambridge University Press, Cambridge, U.K.

[21]   Ehmann, Wm. D. and Vance, Diane, E., 1991. Radiochemistry and Nuclear Method of Analysis. J. Wiley and sons.

[22]   Verren, V. and Hurtgen, C., 2000. A multiple window deconvolution technique for measuring low energy beta activity in samples contaminated with high energy beta impurities using liquid scintillation spectrometry. App. Rad. And Isotopes 53(2000) 289-296.

[23] Fernandez, A. Jose, M. Los Arcos, Grau, A., 1985. A computer program to evaluate the liquid scintillation counting efficiency and its associated uncertainties for K-L atomic shell electron capture nuclides. Computer physics communications. 44, 209-220. North Holland, Amsterdam.

[24] Xiaolin, H. Liquid Scintillation Counting For the Determination of Beta Emitter- Principles and Application, RISO National Laboratory For Sustainable Energy. Technical University of Denmark.

[25] University of Wisconsin: MILWAUKEE Environmental Health Safety And Risk Management Radiation Safety Program.

[26] Allesio, M. Allegri, L. Bella, F. Improta, S., 1978. Influence of quenching on the background of liquid scintillation counters. Nuclear Instruments and Methods. 157, 579-582.

[27] L' Annunziata, M. F., 2003. Nuclear radiation, its interaction with matter and radioisotope decay. Handbook of Radioactivity Analysis (Amsterdam: Academics).

[28] Sprawls,P.,2000. Radioactive transitions. Sprawls Educational foundation, Open Resources for learning and teaching.

[29] Goldbook, 1997. IUPAC Compendium of chemical terminology. 2nd ed. Online Corrected version (2006-) " Auger effect".

[30] Wikipedia, the free encyclopedia: Retrieved from "http//en.wikipedia.org/wiki/Auger effect

[31] Seltzer, S.M. and Berger, M.J.,1982. International Journal of Applied Radiation and Isotopes. 33, 1219.

[32] GrauMalonda A, García-Toraño E. 1982. Evaluation of counting efficiency in liquid scintillation counting of pure beta-ray emitters. International Journal of Applied Radiation and Isotopes 33:249–53.

[33] Pochwalski K, Radoszewski T. 1979. Disintegration rate determination by liquid scintillation counting using triple to double coincidence ratio (TDCR) method.

[34] Simpson, B.R.S., Meyer, B.R., 1992. Direct determination of the activity of non-gamma-emitting radionuclides by the TDCR efficiency calculation technique: a review of the present status. NAC Report/92-02. Faure, South Africa.

[35] GrauMalonda, A. GrauCarles, P.,2001. Free parameter, figure of merit and ionization quench in liquid scintillation. Applied Radiation and isotopes, 54, 447.

[36] Garcia-Toraño E, GrauMalonda A., 1985.EFFY, a new program to compute the counting efficiency of beta particles in liquid scintillators. Computer Physics Communications 36:307.

[37] GrauCarles, P., 2006., EMILIA, the LS counting efficiency for electron capture and capture gamma emitters. Computer Physics Communications 174:43.

[38] Agostinelli, S. Allison, J. Amako, K. Apostolakis, J. Araujo, H. Asai, M. Axen,D. Banerjee, S. Berrand, G. Behner, F. Bellagamba, L. Boudreau, J. Broglia, L.Bronengo, A. Burkhardt, H. Chauvie, S. Chuma, J. Chytracek, R. Cooperman, G., 2003. GEANT4 - A simulation toolkit. Nuclear Instruments and Methods in Physics Research A 506(3): 250-303.

[39] Hamamatsu Corp. 1998. Datasheet of photomultiplier tubes R331-05. Hamamatsu Photonics KK, Japan